

# THERMAL FLUID-STRUCTURE INTERACTION BASED OPTIMIZATION OF SECONDARY AIR FLOWS IN ROTOR STATOR CAVITIES OF AIRCRAFT TURBINES

Hannes Lück<sup>1</sup>, Michael Schäfer<sup>1</sup>, Heinz-Peter Schiffer<sup>2</sup>

<sup>1</sup> Institute of Numerical Methods in Mechanical Engineering

<sup>2</sup> Department of Gas Turbines and Aerospace Propulsion  
Technische Universität Darmstadt, Darmstadt, Hessen 64287

<sup>1</sup>Email: lueck@gsc.tu-darmstadt.de

**Key words:** Thermal Coupling, CFD, FE, Optimization, Aircraft Turbine.

**Abstract.** In aircraft engines, the cooling effectiveness of rotating and stationary turbine discs is sensitive to the provided amount of secondary cooling air. However, the mismatched centrifugal and thermal expansion of turbine discs has to be considered to assess the exact cooling mass flow rate in the relevant rotor stator cavities. This paper discusses two TFSI coupling approaches and an optimization scenario leading to a more effective disc cooling under utilization of coupled Thermal Fluid-Structure Interaction methods. The design variables are statistically evaluated and derivative free and derivative based optimization approaches are compared regarding their efficiency and accuracy.

## 1 INTRODUCTION

The cooling of turbine components like blades and discs is essential since the melting temperatures of the materials used are several hundred degrees below the operating turbine inlet temperature. Cooling air with higher total pressure is required to seal rotor stator cavities and blade surfaces to withstand the hot gases exceeding the combustion chamber. Hereby, up to 20 % of the main annulus flow is bled of the compressor stages and led to the turbine stages around the combustion stage. That quantity of compressed main annulus gas does not enter the combustion chamber and cannot contribute to the overall engine cycle. Therefore, the optimization of these so called secondary air flows is considered to be one of the most promising research activities in gas turbines to enhance the global engine efficiency. The accurate evaluation of the disc metal temperature plays the significant role in predicting component life and the corresponding minimum demand of coolant. Conventional methods conduct finite element analyses and apply semi-empirical correlations of thermal boundary conditions or CFD solutions at the outer disc wall. An enhancement to this pure thermal coupling is the incorporation of thermo-mechanical deformations in a fully coupled Thermal Fluid-Structure Interaction approach (TFSI).

## 2 APPLICATION TEST CASE

The application test case for this work is a turbine test rig from the Turbine Stator Well test facility at the University of Sussex [1]. The two-stage axial turbine rig was built up during the five-year European Union financed research project "Main Annulus Gas Path Interaction" or short MAGPI. The overall objective of the MAGPI project has been to validate and develop computational methods that simulate heat transfer in rotor stator cavities adjacent to the main annulus of gas turbines. The two-stage turbine rig runs at engine representative conditions and is rated at a pressure ratio of 2.7 and 400 kW, resulting in a rotating speed of 10,000 rpm. At the rig design point the main gas mass flow measures 4.9 kg/s at 3 bar and a temperature of 170 °C. Within the MAGPI program, four different cooling flow rates were investigated experimentally and numerically. The lowest cooling flow rate and the case without cooling lead to an ingestion of hot gas while the highest cooling rate results in a total bulk of coolant egress at the rim, each under the cold build and operational state. The cooling flow rate in between these cases is chosen for the present investigations. This cooling rate measures 1.15 % of the main annulus mass flow rate and is most sensitive to TFSI related effects.

The converged TFSI solution is achieved at a hot running geometry that reveals an interstage seal clearance increased by 33 % compared to the cold build state. It is crucial to capture the hot running clearances since the interstage seal flow directly entails the mass flow rate at the rotor stator rim next to the main annulus path. Hereby, the hot running state causes a transition of coolant egress to a slight hot gas ingestion at the rim decreasing the cooling efficiency inside the rotor stator cavity [2].

The default position and orthogonal angle of the cooling entry leads to the core flow with two counter-rotating vortices, which are qualitatively displayed in Figure 1. In case of a hot gas ingestion under hot running condition the coolant only feeds the lower vortex efficiently. Consequently, this default configuration is ineffective in cooling down the whole rotor wall on the left side. An optimized cooling configuration with an angled cooling entry or a different axial cooling position would cool the wall directly and could also benefit from the disc entrainment effect that pumps the air radially outwards. An efficient strategy to find an optimized design shall be discussed in this work.

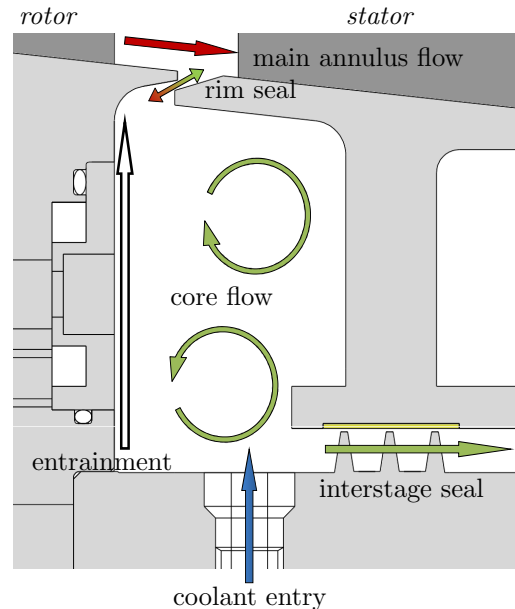


Figure 1: Flow structure in rotor stator cavity of axial two-stage turbine rig

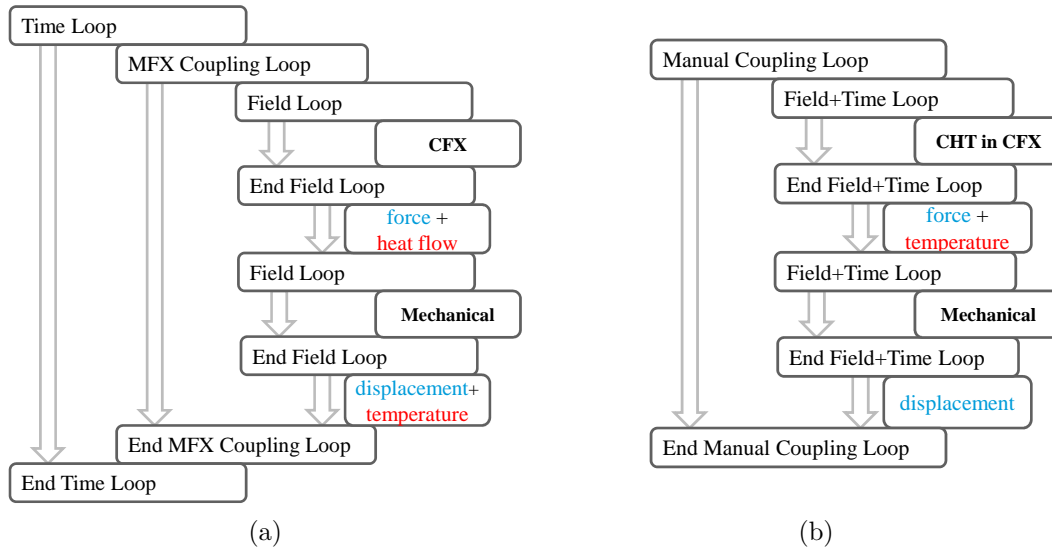


Figure 2: Thermal Fluid-Structure Interaction (TFSI) methods in ANSYS in comparison: (a) Implicit Coupling via the MFX interface and (b) Explicit manual coupling via scripts

### 3 METHODOLOGY

The software package ANSYS offers two different couplings between its CFD solver CFX and FE solver Mechanical. The two couplings can be distinguished as an implicit MFX coupling by utilization of the ANSYS MFX interface and an explicit manual coupling by use of manual scripts. Hereby, the terms implicit and explicit refer to the question when the two solvers exchange variables. The terms MFX and manual coupling target the question where the exchange is located among the fluid and solid domain.

Both coupling types are capable to exchange the thermomechanical variables temperature, heat flux, force and displacement, as displayed in Figure 2. The variable force is disregarded in both approaches since in this context only the fluid forces acting on the solid domain are referred to e.g. the aerodynamic blade load or the pressure differential between cavities. It could be proven that these fluid forces can be neglected because they do not alter the deformations that are caused by centrifugal forces due to the rotation and the thermal expansion due to the high fluid temperatures.

#### 3.1 Implicit MFX coupling

The exchange of the variables in the MFX coupling is located at the fluid-solid interface and is performed implicitly via coupling iterations. The MFX coupling is ought to get initiated with an appropriate CFD solution on the fluid side. With regard to the solid domain, it is not possible to provide a temperature distribution from a stand-alone FE calculation as an initial solution, since a consistent stress-strain state would not match the fluid mesh at the start. Therefore, the convergence rate is solely controlled by the quality of the initial CFD solution and by an adequate choice of under-relaxation factors

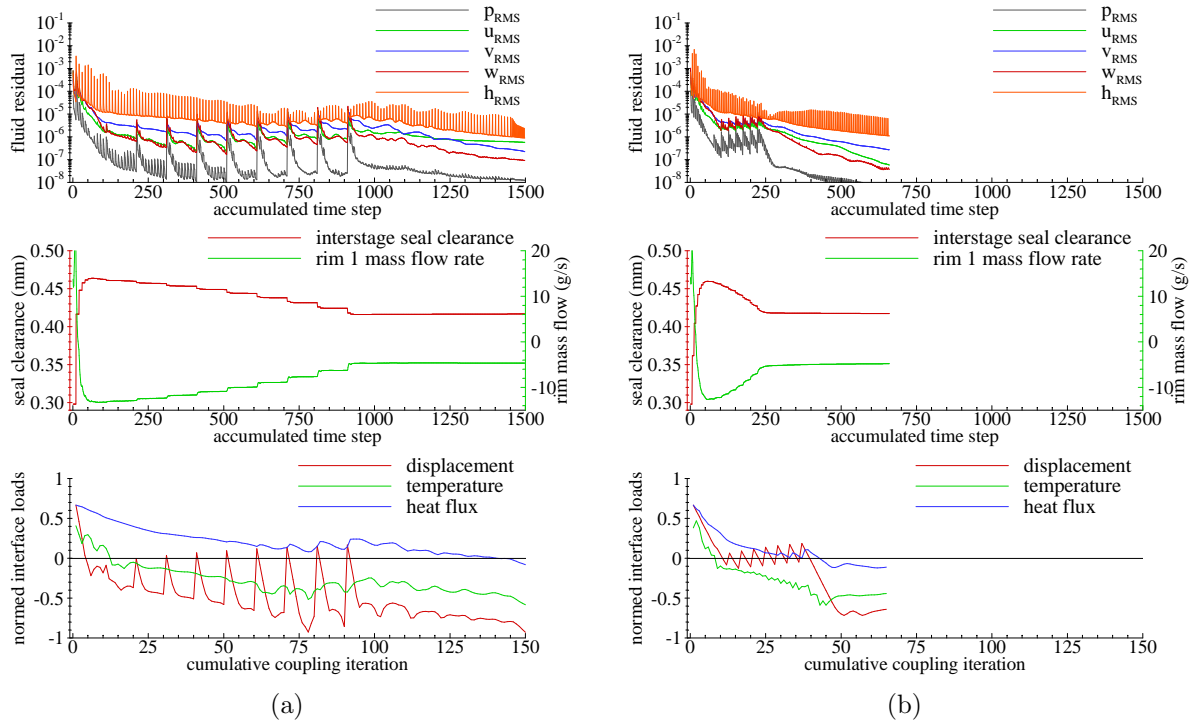


Figure 3: Convergence history for implicit MFX coupling showing fluid residuals, user points and normed interface loads for (a) case 'A' and (b) case 'D' from Table 1

for the interface variables as well as the maximum allowable count of fluid field and coupling iterations. Table 1 lists several MFX settings with the maximum count of coupling iterations and field iterations for the fluid side. Moreover, the relevant under relaxation factors are presented. To begin with, case 'A' is the proposed default setting for FSI cases including heat transfer and takes 28 hours on four CPUs. A strong under relaxation of the interface load heat flux is hereby recommended because it is the most sensitive variable for the overall convergence of the coupling that potentially can induce extreme solid deformations. For the case B, the factor could be set to 0.4. For the investigated application, this is the possible value up to which the factor can be increased before the interface loads diverge. A dynamic adjustment of under relaxation factors during the run is not available. However, this feature would not decrease the runtime significantly, since the under relaxation factors have a much lower impact on the runtime than reduced counts of field and cou-

Table 1: Implicit MFX convergence study

case	A	B	C	D	E
$N_{coup}$	10	10	6	4	2
$N_{time}$	10	10	4	6	8
$URF_{HFLU}$	0.1	0.4	0.4	0.4	0.4
$URF_{DISPL}$	0.75	0.4	0.4	0.4	0.4
$N_{coup,tot}$	145	110	190	43	29
$N_{time,tot}$	1450	1400	780	680	790
runtime (h)	28	26	32	19	16

pling loops as the cases B to E prove. Although the latter parameters impede the already bad convergence within the coupling loop, the overall convergence is reached at an RMS fluid convergence target of  $10^{-6}$ . Especially in case 'E', the 2 coupling loops are not enough to converge the displacement loads at the interface within a false time step. Despite this flaw, also case 'E' reaches the overall convergence and does not diverge.

Figure 3 shows convergence history for the cases 'A' and 'D' by displaying the fluid residuals, two user point data and the normalized interface loads. Despite the optimized choice of MFX parameters for case 'D', the convergence histories of both cases illustrate the problems that arise from the implicit coupling type. Compared to the pure mechanical variables as the deformation or mass flow rates, the enthalpy in the fluid domain and the heat flux at the interfaces converge very slowly. Considering a cavity flow with a Reynolds number of  $2 \cdot 10^6$ , high Mach numbers of 0.6 at the interstage seal fins, and a strong heat convection at the walls, leads to heat transfer problems between the compressible flow and the solids, which are computationally more intensive than the thermomechanical deformation. To sum up, at the current state of development, the MFX coupling solves the Fluid-Structure Interaction in conjunction with high thermal loads very inefficiently.

Apart from that issue, the user points in the history plots reveal the TFSI related improvements of the solution compared to CFD computations on the cold build geometry. As the interstage seal clearance widens up from about 0.3 mm to 0.418 mm, measured radially from the seal fin to the left corner of the stator hub, the rim mass flow rate alters from an coolant egress at around +15 g/s to an ingress of hot gas at around -5 g/s. This ingress of hot gas heats up the cavity flow and impedes the cooling effectiveness of the cavity walls [2].

### 3.2 Explicit manual coupling

The explicit manual coupling has proven to be the more efficient approach since it splits up the thermal coupling between the fluid heat flow and the solid temperatures in a separate CHT (Conjugate Heat Transfer) model from the corresponding calculation of the deformation in the FE solver Mechanical. In a steady-state CHT model it is also possible to assign two different false time steps for the fluid and solid domain respectively, which significantly speeds up the heat transfer process.

In addition to that feature, the manual coupling approach benefits from the access to each evaluation step in an optimization setting as it is displayed in Figure 4. In the original setup of Figure 2b, the first CHT simulation is conducted on the cold build state. The subsequent FE solver is initiated with a solid temperature distribution from the CHT model. The resulting deformed state is exported for every computed solid node in a text file and loaded by the same mesh motion solver that is used in the implicit approach. Subsequent the mesh motion process, the next CHT solution is obtained on the set of deformed fluid and solid meshes.

The converged TFSI solution at the operational state is exactly the same as in the implicit MFX approach. Contrary to the 680 fluid steps within 43 coupling loops for case 'D' in

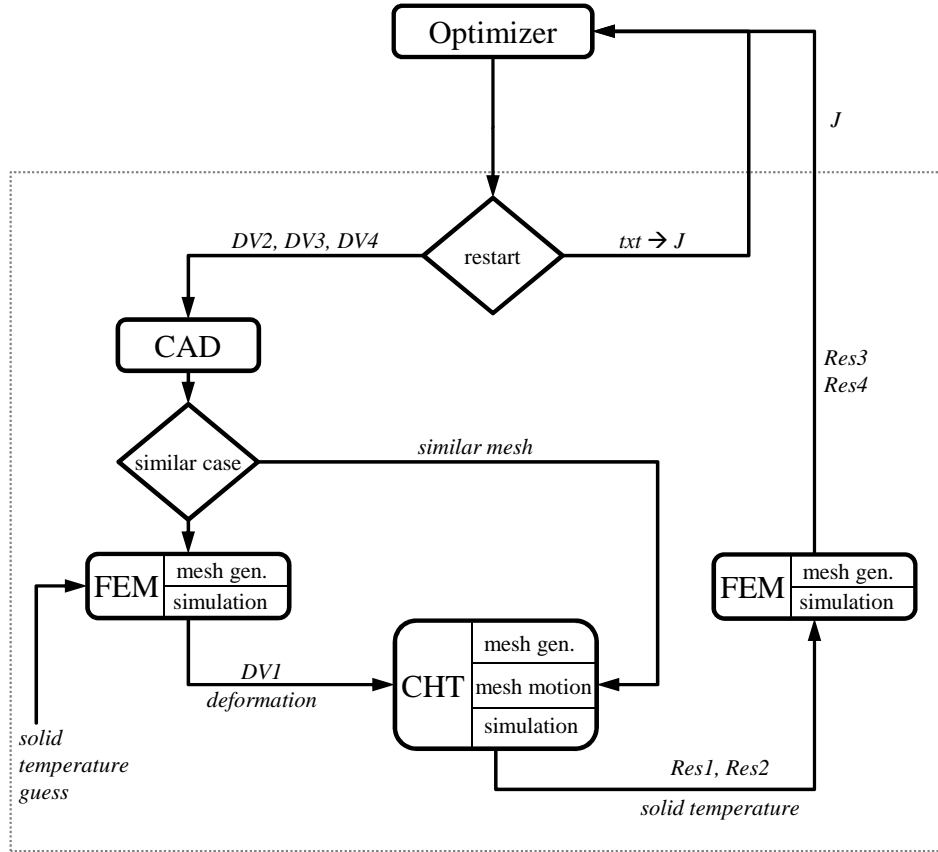


Figure 4: Adjustments for explicit manual TFSI coupling for optimization purposes

Table 1, there are only 400 time steps within two manual coupling loops needed, resulting in two CFX CHT and two Mechanical evaluations. Consequentially, the runtime of 19 hours for the implicit coupling approach is beaten by the runtime of 3 hours for the explicit coupling. Applied on realistic turbine geometries where discs are thinner and cavities are located at higher radii, there are probably more manual coupling loops necessary to reach convergence. However, the manual coupling will be more efficient than the implicit coupling for most turbine cases.

An explanation for the fast convergence and low count of manual coupling loops is that some major components of the presented turbine rig are insensitive to the changes that can be revealed by the TFSI methods. The movement of the stator hub is mainly driven by the rather constant thermal expansion of the casing around the main annulus. Additionally, the deformation of the rotor is dominated by the rotational speed rather than the thermal load. These findings lead to the decision to change the order of solvers to the illustrated adjustment in Figure 4. It is very efficient to apply a solid temperature guess to a first FE calculation since the corresponding deformation guess already leads to a good CHT solution. That arrangement saves at least one manual loop.

## 4 OPTIMIZATION SCENARIO

In context of an optimization scenario, further adjustments help to reduce the computational time of an evaluation e.g. in case of the gradient evaluation during an optimization run, as it is displayed in Figure 4. If two cases of design variables are very similar, the mesh in question can rather be deformed accordingly instead of running the first FE calculation and generating the mesh. That mesh would be then changed on the basis of the deformed state that would not be different for e.g. a slightly adjusted cooling angle. This distinction is displayed by the rhombus 'similar case' in Figure 4. In combination with the very good initial solution this distinction saves up to 60% of the computational time for the evaluation of the gradient information in case of the gradient-based SQP algorithm.

Moreover, it is possible to incorporate the design variables during the FSI evaluation instead of considering every variable in the CAD model at the start. Especially the interstage seal clearance can be split up into a hot running (DV1) and a cold build (Res4) clearance. The latter one is computed as an output of the FSI evaluation while the hot running clearance is implemented in the mesh motion process as a correction of the clearance that is computed in the first FE calculation. Hereby, the first deformation is based on

a solid temperature guess, the design variables DV2-DV4 and the original seal clearance of 0.3 mm. The deformed state is then manipulated at the lower stator hub by several micrometers in order to compute the CHT simulation at the desired hot seal clearance. The resulting solid temperature field is the input for one final FE calculation that determines the actual hot running clearance for this set of design variables. Based on the difference, the consistent cold build clearance is determined which is used as a constraint in the optimization scenario since the cold build clearance cannot fall below a critical value of 0.18 mm. This value is determined as the maximal radial expansion of the rotor at a worst case scenario with higher rotational speed and thermal load.

The essential advantage of this choice of design variables is that only two FE and one CHT calculations are needed to evaluate one TFSI solution. This saves at least one CHT

- DV1 hot running seal clearance
- DV2 axial cooling position
- DV3 cooling angle
- DV4 radial cooling position
- Res1 rotor inner wall temperature
- Res2 rim mass flow rate
- Res3 maximum von-Mises stress
- Res4 cold build seal clearance

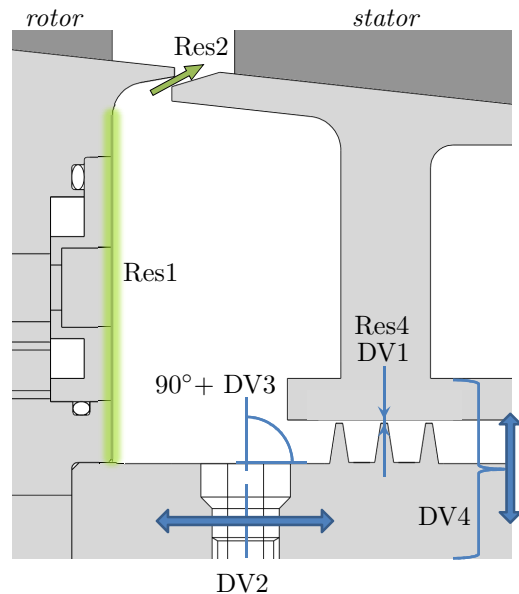


Figure 5: Design variables and Results (Res3 is measured close to the shaft)

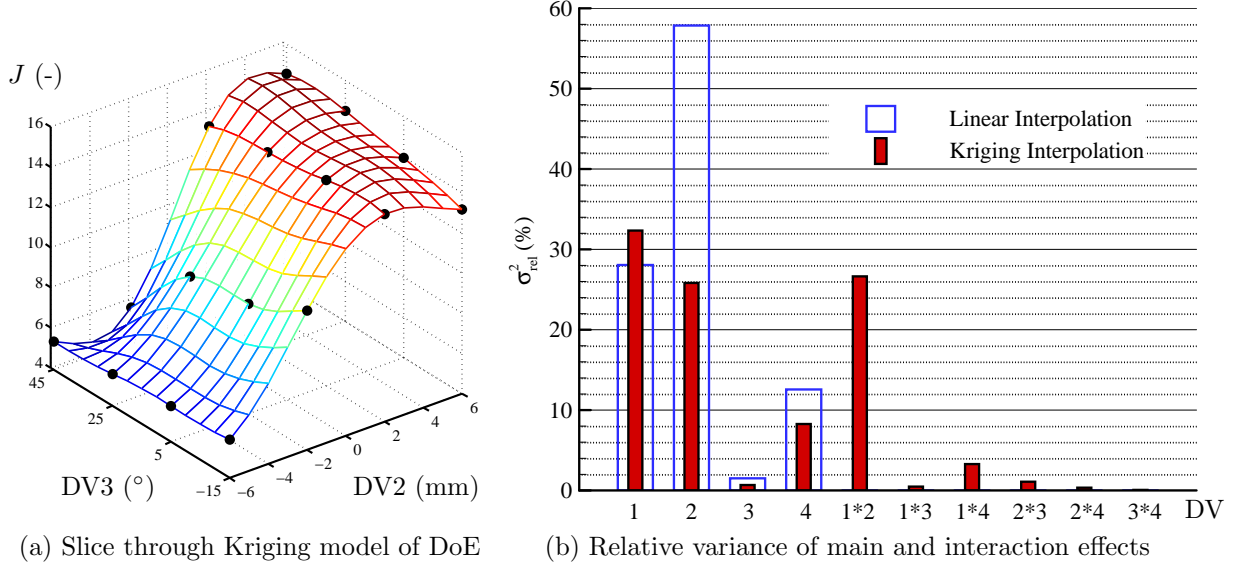


Figure 6: (a) Slice through nonlinear Kriging model of full factorized  $4^4$ -points DoE (Slice for default DV4 and maximum DV1=0.450 mm) and (b) relative variance of main and interaction effects based on metal model interpolated by linear and nonlinear fit

evaluation in comparison to the original setup in Figure 2b. Additionally, this optimization scenario is well-posed by the interstage seal correction within the evaluation, since this strategy decouples the first design variable from the other design variables.

The optimization scenario aims for an optimized cooling and minimized stresses in the rotative assembly at a specified slight egress of coolant at the rim. These goals are the displayed as Res1-Res3 in Figure 5. The objective function  $J$  is split up in three goals

$$J = 10 \cdot \left( \frac{1}{3} \cdot \frac{|\text{Res1} - J_1|}{\Delta\text{Res1}} + \frac{1}{3} \cdot \frac{|\text{Res2} - J_2|}{\Delta\text{Res2}} + \frac{1}{3} \cdot \frac{|\text{Res3} - J_3|}{\Delta\text{Res3}} \right), \quad (1)$$

$$\begin{array}{lll} J_1 = 90 \text{ }^\circ\text{C} & J_2 = 7 \text{ g/s} & J_3 = 4.6 \text{ MPa} \\ \Delta\text{Res1} = 20 \text{ }^\circ\text{C} & \Delta\text{Res2} = 12 \text{ g/s} & \Delta\text{Res3} = 0.6 \text{ MPa} \end{array}$$

which are defined as the temperature at the rotor wall, normed by the potential temperature drop, plus the mass flow, normed by the desired mass flow rate at the rim and the maximum stresses in the rotative assembly, normed by the potential stress reduction. The factor of 10 at the beginning of the equation 1 is set to lift the objective value to the same scale as the design variables, which are also scaled and corrected at the beginning of the TFSI evaluation. The manual TFSI approach is coupled with the MATLAB optimization toolbox using algorithms such as the gradient-based sequential quadratic programming (SQP) and the gradient-free Nelder-Mead simplex algorithm. In order to investigate the performance of the chosen optimizer, a full factorized Design of Experiments (DoE) with 256 evaluations is additionally conducted to build a linear model and a non-linear Kriging model. The nonlinear model enables the determination of the global minimum for  $J$ .

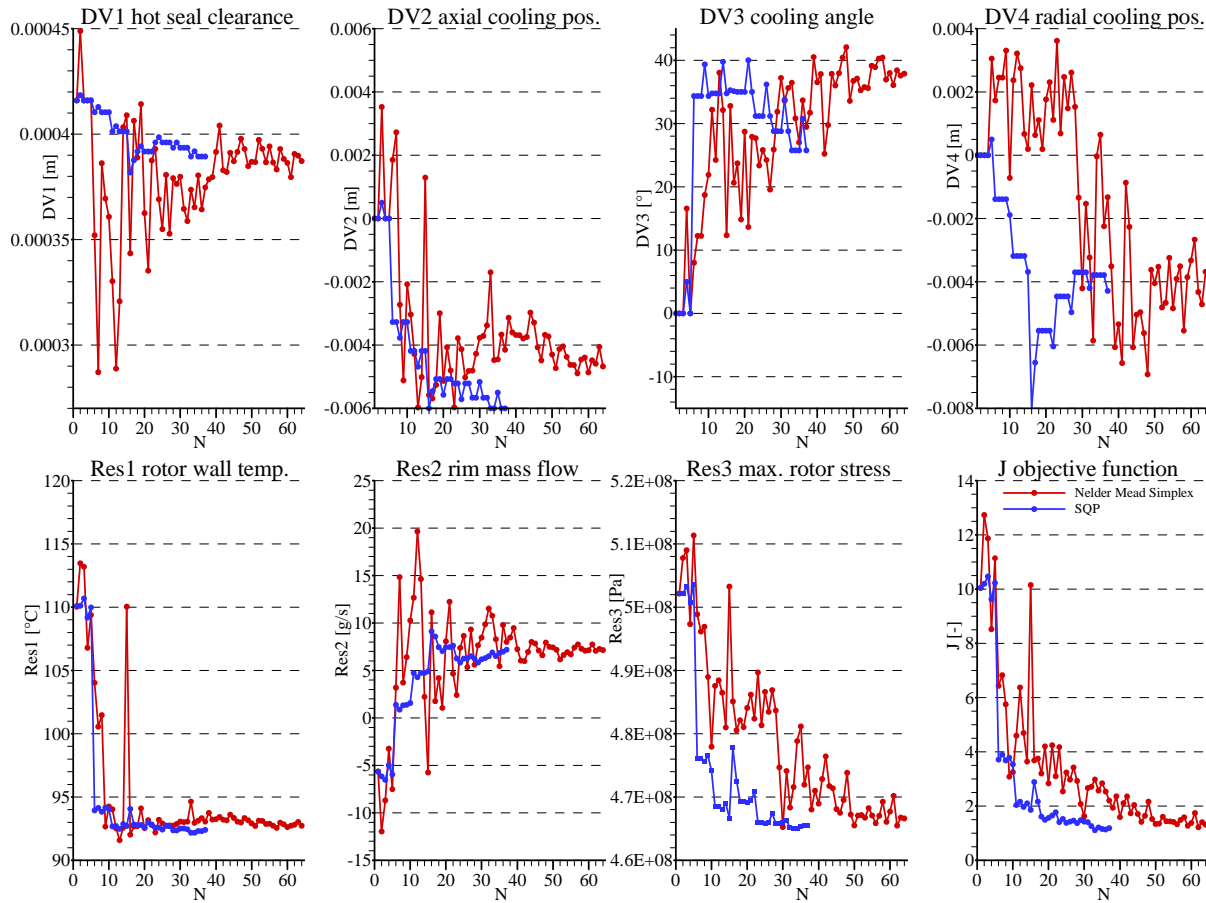


Figure 7: Optimization scenario for 2D axisymmetric surrogate model: Comparison of gradient-based SQP and gradient-free bounded Nelder-Mead algorithms

Moreover, it is possible to statistically assess the utilized design variables [3]. Hereby, an analysis of variance illustrates the poor credibility of a linear model compared to the non-linear Kriging model in Figure 6b. The linear model does not reproduce any interaction effects between the design variables. Moreover, the sensitivity of the objective function towards the design variable 2, which is the axial cooling position is exaggerated by the factor of 2. Figure 6b also reveals the small impact of the cooling angle (DV3) compared to the other parameters, which is exemplary illustrated by Figure 6a.

Figure 7 compares the two investigated optimization algorithms. The Nelder-Mead Simplex algorithm is an advanced version of the original MATLAB code that can operate in the given geometrical bounds by mapping each parameter range on an 'arctan' function. This modification enables the algorithm for the given application. The algorithm is also chosen since a objective function that is based on the simulation of heat transfer problems tend to be noisy due to the slow convergence rate and sometimes overhasty, alleged termination. This noise could degrade the gradient information in gradient-based algorithm. Several adjustments to the SQP algorithm showed that the noise is low and

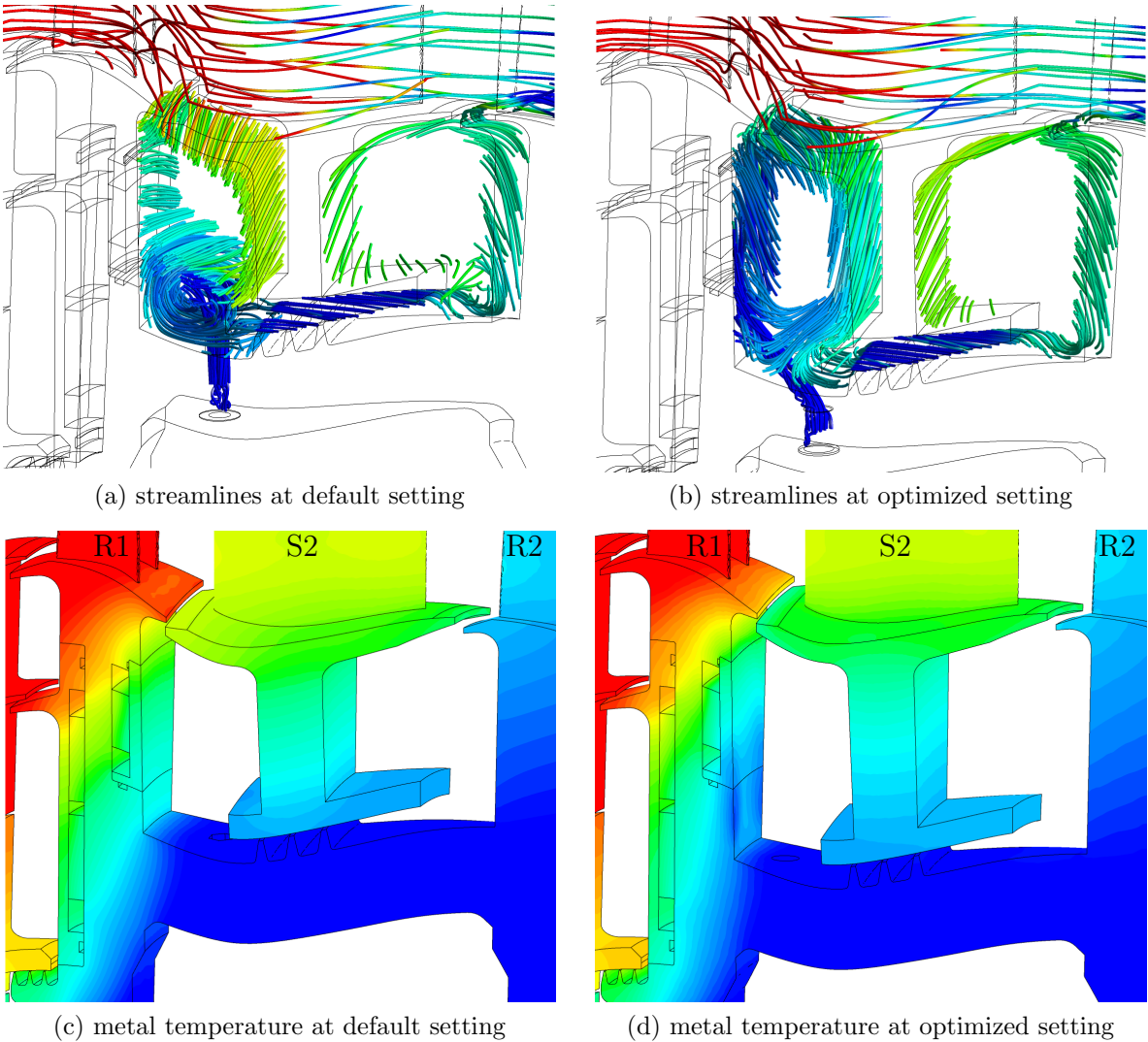


Figure 8: Comparison of default and optimized setting: (a+b) streamlines with fluid temperature and (c+d) metal temperatures, each on individual normalized scales

can be overleaped by slightly increasing the step size for the gradient forward differencing scheme. The comparison of both algorithm proves the efficiency of the gradient-based SQP algorithm, which needs only half of the evaluations than the Nelder-Mead, which are additionally significantly cheaper because of the discussed adjustments to the manual TFSI coupling. Both algorithms reach a very similar  $J$  goal although the two design variables DV2 and DV3 turn out to have different optimal values. The difference can be explained by the applied modifications for the Nelder-Mead simplex algorithm which prevents the optimizer from running against the bounds. Nevertheless, its axial cooling position that is not as close to the wall as in the SQP evaluation is accounted for by a higher cooling angle that is more directed towards the wall. Thus, both settings result in the same wall temperature, rim mass flow rate and objective value. The resulting effect

of the optimized setting on the 3D sector model is illustrated by Figure 8. All design adjustments lead to the almost same improvements as in the 2D surrogate model. The whole cavity is sealed at the same egress of coolant at the rim, the wall metal temperature is significantly decreased due to the simplified core flow and more directed cooling jet and the modified radial position reduces the centrifugal load on the rotative assembly.

## 5 CONCLUSION

An efficient optimization strategy is presented, which utilizes a manual coupling between a CHT and FE solver, separating the solution of the heat transfer from the corresponding deformation. This manual coupling has proven to be more efficient than the MFX coupling that exchanges the thermomechanical variables implicitly at the fluid-solid interface and solves the heat transfer in parallel to the stress-strain state.

A set of four design variables is chosen to optimize the cooling efficiency in a rotor stator cavity of a turbine rig. The non-linear effect of the design variables on the objective function could be assessed by a Kriging meta-model and important interaction effects between design variables are revealed by an analysis of variance. The gradient-based SQP method is affirmed to be the superior optimization technique in comparison to the gradient-free Nelder-Mead simplex algorithm, which reaches the optimization goal in twice as many evaluations and significantly longer computational time.

## ACKNOWLEDGMENT

The authors would like to thank Christopher Long from the Thermo-Fluid Mechanics Research Centre at the University of Sussex as well as Jeffrey Dixon from Rolls-Royce plc for their support and permission to use the rig geometry for the presented investigations. This work is supported by the German Research Foundation, in particular the Research Training Group 1344, and by the 'Excellence Initiative' of the German Federal and State Governments and the Graduate School of Computational Engineering at Technische Universität Darmstadt.

## REFERENCES

- [1] Coren, D. D., Atkins, N. R., Turner, J. R., Eastwood, D. , Childs, P. R. N., Dixon, J. A., and Scanlon, T. S.. An advanced multi-configuration stator well cooling test facility. *In Proceedings of ASME Turbo Expo 2010*, GT2010-23450.
- [2] Lück, H., Schiffer, H.-P., Schäfer, M.. Simulation of thermal fluid-structure interaction in blade-disc configuration of an aircraft turbine model. *In Proceedings of ASME Turbo Expo 2014*, GT2014-26316.
- [3] Harzheim, L.. *Strukturoptimierung: Grundlagen und Anwendungen*. (2008)